

Cryo-electron Tomography of Clathrin-coated Vesicles: Structural Implications for Coat Assembly

Yifan Cheng^{1*}, Werner Boll², Tomas Kirchhausen²
Stephen C. Harrison³ and Thomas Walz¹

¹Department of Cell Biology
Harvard Medical School
240 Longwood Avenue, Boston
MA 02115, USA

²Department of Cell Biology and
CBR Institute for Biomedical
Research, Harvard Medical
School, 200 Longwood Avenue
Boston, MA 02115, USA

³Howard Hughes Medical
Institute and Department of
Biological Chemistry and
Molecular Pharmacology
Harvard Medical School
250 Longwood Avenue
Boston, MA 02115, USA

Clathrin-coated vesicles mediate vesicular traffic in cells. Three-dimensional image reconstructions of homogenous populations of *in vitro* assembled clathrin coats have yielded a molecular model for clathrin and its interactions with some of its partners. The intrinsic averaging required for those calculations has precluded detailed analysis of heterogeneous populations of clathrin-coated vesicles isolated from cells. We have therefore used cryo-electron tomography to study the lattice organization of individual clathrin-coated vesicles and the disposition of the captured vesicle with respect to the surrounding coat. We find a wide range of designs for the clathrin lattice, with different patterns of pentagonal, hexagonal, and occasionally heptagonal facets. Many coats, even smaller ones, enclose membrane vesicles, which are generally offset from the center of the clathrin shell. The electron density distribution between the coat and the underlying vesicle is not uniform, and the number of apparent contacts that anchor the clathrin lattice to the vesicle membrane is significantly less than the number of clathrin heavy chains in the assembly. We suggest that the eccentric position of the vesicle reflects the polarity of assembly, from initiation of coat formation to membrane pinching.

© 2006 Elsevier Ltd. All rights reserved.

Keywords: clathrin; clathrin-coated vesicles; endocytosis; cryo-electron tomography; cryo-electron microscopy

*Corresponding author

Introduction

Clathrin-coated vesicles are specialized organelles that carry endocytic membrane traffic from the plasma membrane to endosomes and secretory traffic between the trans-Golgi network and endosomes;^{1,2} they also participate in synaptic vesicle recycling.³ Clathrin, the protein that forms the lattice-like coat of these structures, is a spider-like trimer (a triskelion), with three legs radiating from a central hub. Adaptor proteins link the clathrin scaffold to the enclosed membrane vesicle and to membrane-anchored cargo proteins.^{1,4–6}

The formation of clathrin-coated vesicles follows a sequence of coordinated steps, in which membrane invagination is coupled to growth of the

clathrin lattice, leading to lattice closure and vesicle budding.^{1,7,8} Early electron microscopy (EM) studies of negatively stained clathrin-coated vesicles purified from pig brain showed coats with a wide variety of designs accommodating vesicles of different sizes and shapes.⁴ *In vitro* assembled clathrin lattices^{9–11} can have more uniform and symmetrical designs (e.g. lattices with icosahedral, D6 or tetrahedral symmetry), particularly if assembled with the endocytic adaptor protein complex AP-2. A recent study based on cryo-electron microscopy of clathrin/AP-2 coats imaged in vitrified ice produced electron density maps at sub-nanometer resolution, obtained from averaged images of these structures.¹² When combined with the atomic structures of individual clathrin domains,^{13,14} these maps yielded a molecular model for a clathrin lattice.¹² The approach was extended to the analysis of how auxilin, the co-factor required for the Hsp70 and ATP-dependent dissociation of the coat, interacts with clathrin within the lattice.¹⁵

Clathrin-coated vesicles purified from tissues contain many protein components in addition to

Present address: Y. Cheng, Department of Biochemistry & Biophysics, University of California San Francisco, 600 16th Street, San Francisco, CA 94158, USA.

E-mail address of the corresponding author:
ycheng@biochem.ucsf.edu

adaptors, mostly in sub-stoichiometric ratios with respect to clathrin, and our understanding of their disposition with respect to the encapsulated, cargo-carrying lipid vesicles remains largely inferential. We describe here reconstructions of individual coated vesicles obtained by cryo-electron tomography. Even the smallest of the many lattices we detect can enclose a vesicle, which has an unexpected eccentric disposition with respect to the surrounding coat.

Results and Discussion

Cryo-electron tomography of single clathrin-coated vesicles

Clathrin-coated vesicles were purified from bovine brain,¹⁶ using a gentle isosmotic procedure to prevent membrane shrinkage,¹⁷ and embedded in vitreous ice. Cryo-electron microscopy images (Figure 1(a)) of these frozen hydrated coated vesicles recorded with a conventional low dose of $\sim 20e^-/\text{\AA}^2$ show that the individual assemblies differ in size

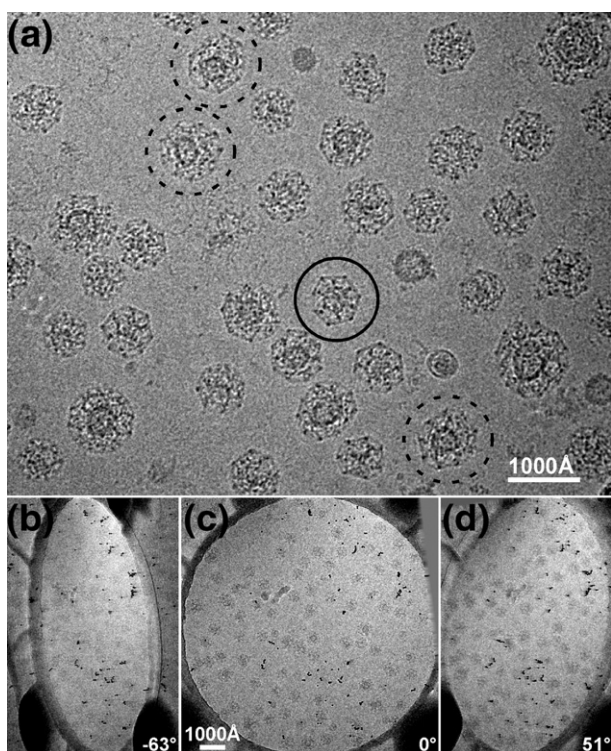


Figure 1. (a) Cryo-electron microscopy image of clathrin-coated vesicles embedded in vitreous ice. The particle marked by a continuous circle is probably the top view of a D6 barrel. From the projection image alone, it is difficult to determine whether the coat contains a vesicle. The particles marked by broken circles are larger and contain vesicles obviously offset from the centers of the coats. (b)–(d) Three representative raw images of a tilt series used to calculate cryo-tomograms of vitrified clathrin-coated vesicles. The tilt axis is approximately along the vertical direction.

and shape, and that many contain membrane vesicles. These preparations contain all the assembly components: clathrin triskelions, adaptor protein complexes, membrane vesicles and possibly cargo proteins trapped within the vesicles (data not shown). Because of their obvious heterogeneity, we could not use single-particle averaging (as used to reach sub-nanometer resolution from images of reassembled coats¹²) to analyze these structures, and we have therefore used cryo-electron tomography to obtain 3D reconstructions of individual frozen hydrated coated vesicles at lower resolution.

Images in a tilt series (Figure 1(b)–(d)), recorded as described in Materials and Methods, were aligned with each other to calculate the electron tomograms. Figure 2(a) shows a central section from a reconstructed tomogram of a vitreous ice slab with embedded clathrin-coated structures. The membrane vesicles are clearly visible within many of the coats (arrow heads). One of them (circled in Figure 2(a)), boxed out from the tomogram, is presented as a series of sequential parallel 62 Å thick slices (Figure 2(b)). Comparison with similarly sliced views of an empty clathrin coat boxed out from the same field (Figure 3) makes it clear that the particle shown in Figure 2(b) is indeed a vesicle surrounded by a clathrin coat. The continuous membrane of the vesicle and the lattice of the coat (especially its relatively highly contrasted vertices) are all clearly visible. It has been suggested that coats smaller than the icosahedral “soccer ball” might not be able to accommodate a membrane vesicle.¹⁸ Without a full reconstruction, it has not been possible to test this proposal, because it is difficult to distinguish between a coated vesicle and a reassembled empty coat with randomly captured protein content. The tomographic reconstructions here show that even the smallest lattices we have isolated often contain membrane vesicles. The vesicle in Figure 2(b) is spherical, with a mean diameter of about 340 Å; the clathrin lattice has an outer diameter of about 700 Å.

The 3D density map of this coated vesicle (Figure 2(c)), viewed along the ice slab and perpendicular to the tilt axis, shows that the missing wedge effect leads to non-uniformity in the resolution of the tomographic 3D reconstruction.¹⁹ The details in the equator of the reconstruction are substantially sharper than at its top and bottom. The representation of the vesicle membrane is continuous in the vicinity of the equator but broken axially, and the reconstructed image elongates perpendicular to the vitreous-ice slab. Nevertheless, the pentagons and hexagons of the clathrin lattice on the surfaces of the assemblies, including the top and bottom of the reconstruction, are all well resolved (Figure 2(b) and (c)). The density surrounding the membrane vesicle divides into two layers (Figure 2(d)). The outer layer clearly defines the hexagons and pentagons of the clathrin lattice. The much higher (~ 8 Å) resolution images obtained from single-particle averaging of *in vitro* assembled clathrin coats show that the hexagonal and pentagonal edges of the polyhedron are

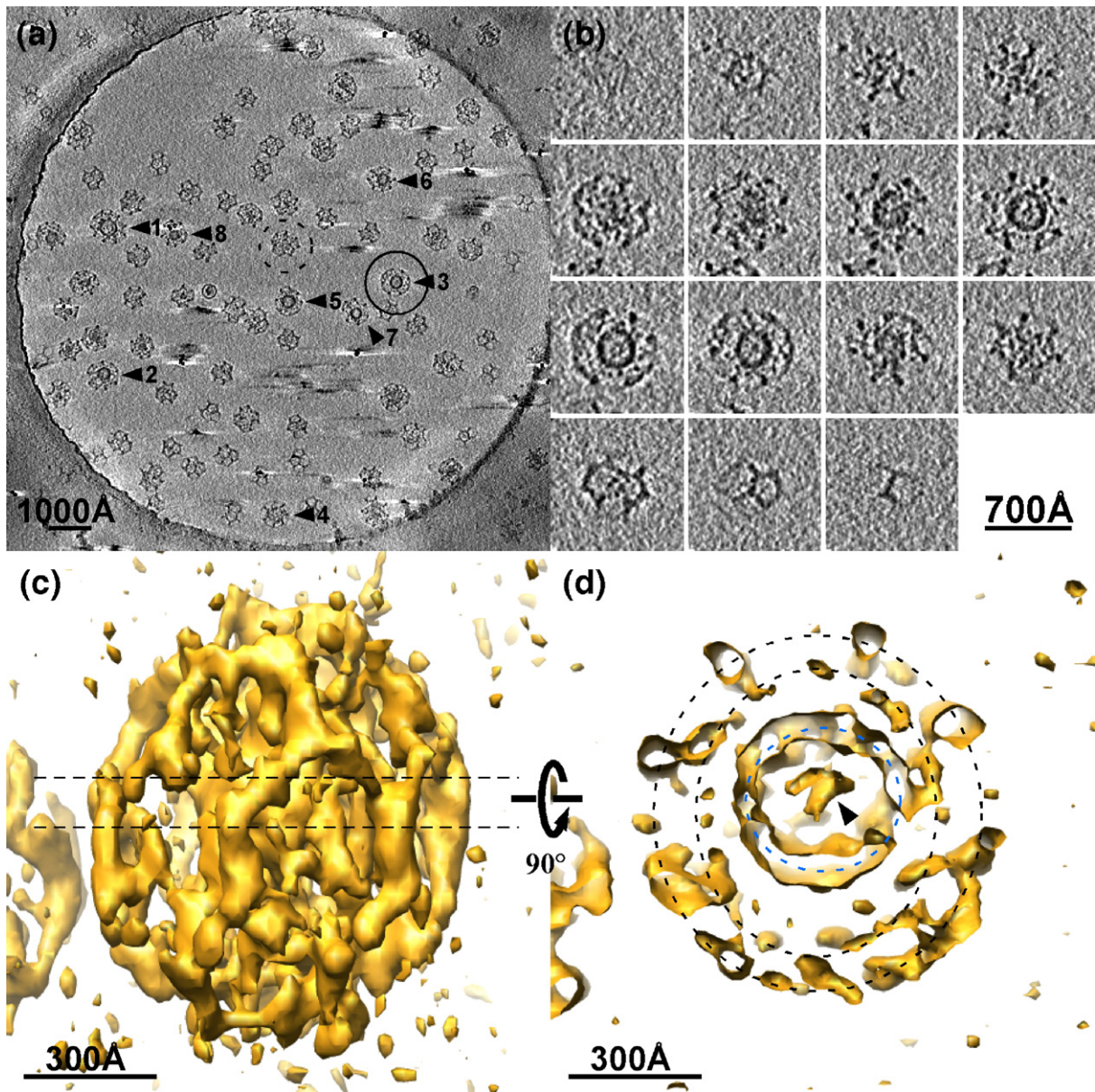


Figure 2. Tomography of clathrin-coated vesicles. (a) Central section (155 Å thick) of an electron tomogram of coated vesicles embedded in a slab of vitreous ice over a hole in a carbon film. The diameter of the hole is 1 μm. (b) Slices through a single coated vesicle (circled in (a), and particle 3 in Figure 4). The slice thickness is 62 Å. (c) Isodensity surface for the coated vesicle shown in (b) viewed from the side. (d) Central section of the same density map, corresponding to the broken lines in (c), viewed from the top. The black broken circles mark the locations of two separate layers of density that surround the vesicle; the blue broken circle marks the membrane of the vesicle itself.

bundles (about 70 Å in diameter) of two anti-parallel clathrin heavy-chain proximal segments (each with an associated light chain) and two anti-parallel distal segments.¹² Therefore, the inner density layer in the tomographic reconstruction must correspond to the heavy-chain N-terminal domains and linkers; it is weaker than the outer layer and less defined in its features. There appear to be some connections between the inner layer and the vesicle membrane. The membrane vesicle is of uniform curvature with a relatively smooth surface, except where contacts from the clathrin coat impinge. Adjusting the threshold of the 3D density map reveals within the vesicle a feature, perhaps protein cargo, connecting

to the membrane opposite a position where inner-layer density from the clathrin coat makes contact. Density inside the vesicle varies from particle to particle, but the inner spaces of these brain-derived coated vesicles are clearly not crowded.

Clathrin lattices

We have analyzed in detail the tomographic 3D reconstructions of eight individual coated vesicles (Figure 4(a) and (b)). The lattices, reconstructed without ambiguity, show different designs, ranging from 36 to 60 triskelions (Table 1). The smallest (36 triskelions) has the so-called tennis-ball structure,⁴

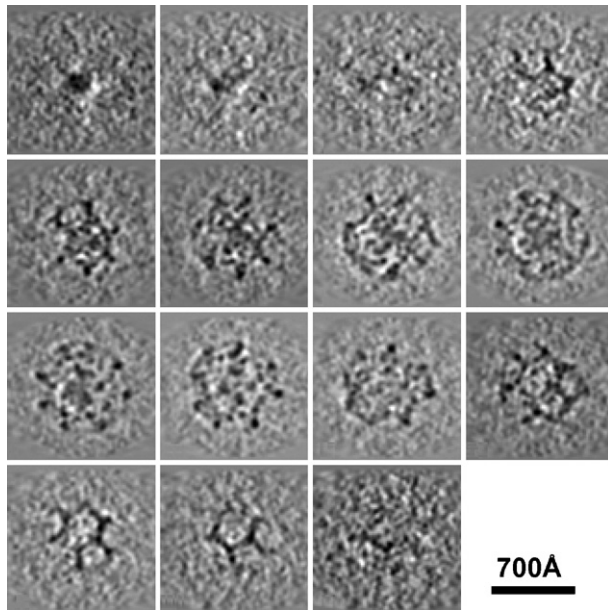


Figure 3. Slices through a single clathrin coat that does not contain a membrane vesicle. Coats like this are probably assembled spontaneously from clathrin triskelions during the purification process.

with D2 symmetry (particle 8 in Figure 4(b)). The number of triskelions is the same as in the D6 barrel, frequently found in clathrin coats assembled *in vitro*, but the 12 pentagons form a continuous chain, like the seam of a tennis ball, rather than two distinct rings of six. The vesicle inside this tennis-ball coat has a diameter of about 310 Å. The largest lattice (particle 1 in Figure 4(b)) has the same number of triskelions as does an icosahedral coat. The coat of particle 1, like that of particle 4 in Figure 4(b), contains a heptagon and 13 pentagons. In a lattice composed entirely of hexagons and pentagons, exactly 12 pentagons are needed to form a closed shell. Inclusion of one or more heptagons requires a corresponding number of additional pentagons. Heptagons have been observed in clathrin lattices, especially near edges of the flat clathrin arrays that form where fibroblasts in culture make contact with the substrate on which they are growing.²⁰ Of the two heptagons in the eight structures described here, one is surrounded by six pentagons and one hexagon and the other is surrounded by four pentagons and three hexagons. In both lattices, the heptagon creates a larger opening as well as a larger radius of curvature in the coat.

Contrary to our expectations, we found that most of the lattices shown in Figure 4(b) lack overall symmetry (the tennis ball with D2 symmetry is an exception), and they deviate in different degrees from a spherical shape. The deviations of the coats from a circular outline come not from the inevitable distortion of a tomographic reconstruction with a missing wedge, but rather reflect the designs of the clathrin lattices themselves. Surface tension or other physical forces are unlikely to have produced the

departure from an overall spherical shape, as the distortions appear in all orientations even though the illustrations in Figure 4(b) are oriented so that the direction of view is always perpendicular to the surface of the ice.

Interactions between coats and vesicle membrane

The density of the inner layer of the coat is not as well defined as that of the lattice-like outer layer. We can nonetheless identify, especially near the equator where missing-wedge effects are least, connections between inner-layer features and the membrane vesicle within (see asterisk (*), Figure 5(a)). These are presumably positions at which the N-terminal domains of clathrin and AP-2 adaptor proteins (or other proteins) come together in the vicinity of the lipid bilayer. It is difficult to determine how many contacts of this kind are present in any one of the coated vesicles studied here, because of the relatively noisy electron density at the top and bottom of the 3D reconstructions. Nevertheless, these contacts are clearly resolved around the equators (Figure 6), and in some cases they contain a sufficiently large volume to accommodate a heterotetrameric adaptor complex (Figure 7).

Figure 5(b) shows an equatorial section of the 3D reconstruction in Figure 5(a), together with the

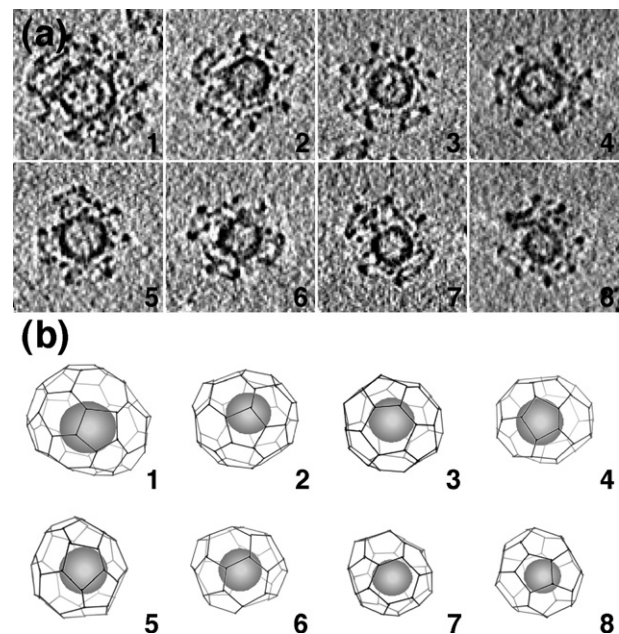


Figure 4. Outline of clathrin lattices in individual coated vesicles. (a) The particles correspond to the clathrin-coated vesicles indicated in the tomogram shown in Figure 2(a). The images correspond to central sections (62 Å thick) viewed from the top. (b) Clathrin lattices were determined by manual tracing along the electron density of the individual tomograms. The spheres inside the lattices represent the sizes and locations of the membrane vesicles contained within each coat. The views are presented in the same orientation as the central sections of the coated vesicles in (a).

Table 1. Reconstructed clathrin lattices from the cryo-electron tomogram of coated vesicles

	Number of edges	Number of triskelions	Number of pentagons	Number of hexagons	Number of heptagons	Vesicle diameter (Å)
1:	90	60	13	18	1	500
2:	75	50	12	16	0	390
3:	66	44	12	12	0	370
4:	60	40	13	8	1	400
5:	60	40	12	10	0	370
6:	57	38	12	9	0	360
7:	57	38	12	9	0	340
8:	54	36	12	8	0	310

Vesicles 6 and 7 have the same number of triskelions, but the lattices are mirror images of each other.

atomic structures of clathrin triskelions (in red) placed into that reconstruction. The fit confirms our assignment of the inner density layer to the N-terminal domains of the clathrin heavy chains. The eccentric position of the vesicle brings these terminal domains into contact with densities anchored on the membrane. On the left-hand side of the image, there is a gap of 50–100 Å between the vesicle membrane and the terminal domains, and the vesicle surface is rather smooth on that side, except for one extended connection. A similar gap between the vesicle membrane and the N-terminal domains of clathrin heavy chains can be detected in others of our tomographically reconstructed coated vesicles (Figure 6). As seen in Figure 4(a) and (b), and Table 1, the diameter of the membrane vesicle is generally proportional to the number of the triskelions in the assembly, but the relationship is not a strict one. The vesicle inside lattice 4 is slightly larger than the vesicles inside lattices 2 and 3, which have more triskelions (Table 1). As a result, the vesicles in 2 and 3 are encased more loosely, with more obvious gaps between coat and membrane.

In the smallest structure analyzed here (8 in Figure 4), with 36 clathrin triskelions and hence 108 heavy chains, the membrane vesicle has a diameter of

about 310 Å. If tightly covered, its surface could accommodate a total of about 30–40 AP-2 complexes, but the reconstruction shows clearly that such a dense coating is not present. We can conclude that the total number of AP-2-mediated contacts between the clathrin coat and the vesicle membrane is substantially less than the total number of clathrin heavy chains in the lattice.

Most of the coated vesicles in our tomogram probably correspond to precursors of synaptic vesicles.²¹ The eccentric locations of the vesicles inside the coats are more obvious than in larger coated vesicles observed by electron microscopy of thin sectioned tissues,²² in part because the difference between the maximum and minimum vesicle-to-coat spacing is easier to detect in these highly curved structures. To confirm that this eccentricity is not a property of vesicles that have uncoated and then recoated during isolation, we prepared coated vesicles from bovine brain by essentially our standard procedure (see Materials and Methods), but isolated and purified at somewhat higher ionic strength and pH (25 mM NaMes (pH 7.0), 100 mM NaCl, 1 mM EGTA, 0.5 mM MgCl₂), to minimize even more the possibility of reassembly and artificial recoating of synaptic vesicles.²¹ We recorded

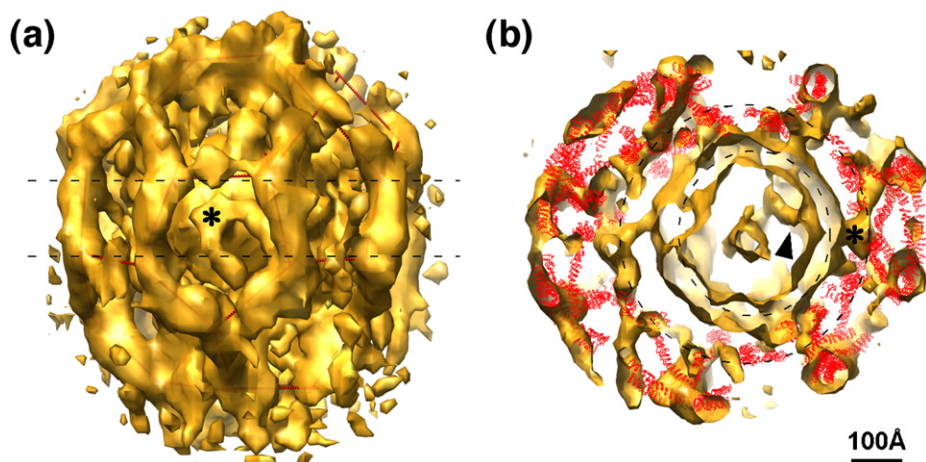


Figure 5. Details of coated vesicle 4 from Figure 4. (a) Surface-rendered density map; the asterisk (*) marks a feature anchored in the vesicle membrane. Red lines within the density outline the lattice. (b) Central section of the same density map, with the ribbon diagrams of vertices of a clathrin lattice positioned within it. The two broken circles represent the vesicle membrane (smaller circle) and the radial location of the N-terminal domains of the clathrin heavy chains (larger circle).

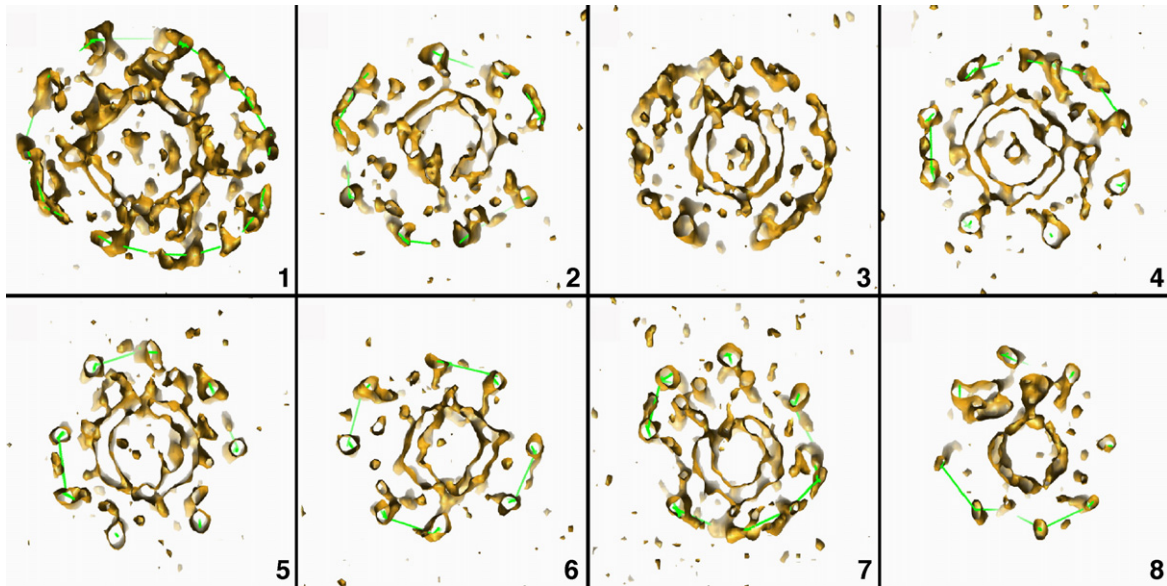


Figure 6. Central sections of the tomographic density maps of each of the eight coated vesicles shown in Figure 4, illustrating the eccentric positions of the membrane vesicles and the positions of the N-terminal domains of the clathrin heavy chains with respect to the vesicles.

untilted cryo-electron microscopy images of these particles and examined a number of fields; many particles are still seen to have the vesicle off-center within the coats (Figure 8(a) and (b)).

We suggest that the eccentric position of the vesicle within the coat comes from the polarity of initiation and completion of the lattice. The positions of close contacts of lattice and vesicle may correspond to preferential locations of adaptors and other proteins that mark the region within a coat at which assembly began, as concluded from recent live-cell imaging studies (S. Saffarian and T. K., unpublished results). Unlike initiation, completion of a clathrin lattice, which occurs *in vitro* even when no vesicle is

present, does not require membrane contact by clathrin.

In summary, cryo-electron tomography has allowed us to relate the structural properties of authentic coated vesicles to molecular details derived from higher-resolution methods. The reconstructed images shows that coats containing as few as 36 triskelions (e.g. the tennis-ball structure and, presumably, the D6 barrel) can engulf a membrane vesicle of just over 350 Å diameter, similar to the observed diameter of neurotransmitter-loaded synaptic vesicles.²³ The variety of lattices in a single preparation is consistent with assembly by sequential incorporation of individual clathrin

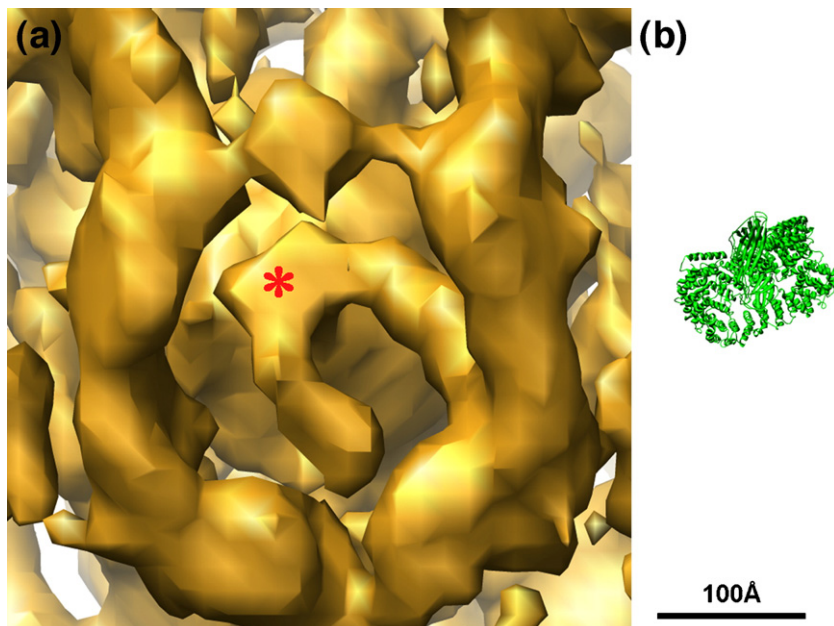


Figure 7. (a) Enlarged view of Figure 5(a), showing a feature anchored on the vesicle membrane. (b) Ribbon diagram of the AP-1 core structure (PDB code 1W63)²⁹ at the same scale as the density map. The size of the AP-1 core matches the size of the density anchored on the membrane in (a).

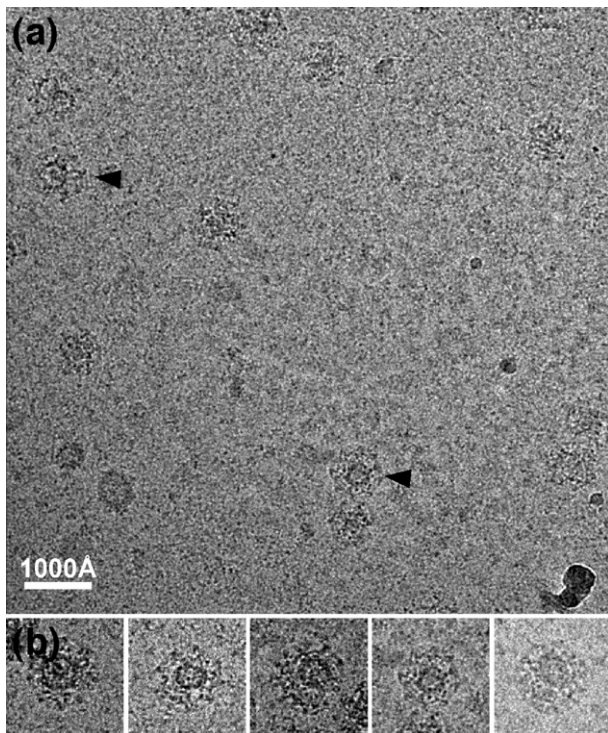


Figure 8. (a) A cryo-electron microscopy image of clathrin-coated vesicles embedded in vitreous ice. The coated vesicles were purified at high ionic strength and pH to prevent recoating during purification. Vesicles within two of the coats (arrow head) are obviously eccentric. (b) A gallery of selected clathrin-coated vesicles boxed out from various areas of the sample.

triskelions, as postulated from live-cell imaging data on the kinetics of coat formation.⁸ A defined region of close association between the membrane bilayer and the protein shell may mark the position at which assembly was initiated, and further analysis may therefore provide evidence for how coat formation starts.

Materials and Methods

Sample preparation and data collection

Clathrin-coated vesicles were isolated from bovine brain¹⁶ and subjected to a final purification step by equilibrium centrifugation for 20 h (at 112, 700g) of the crude coated vesicles applied to the top of a linear gradient ranging from 2% (v/v) Ficoll, 9% (v/v) ²H₂O to 20% Ficoll, 90% ²H₂O in isolation buffer.¹⁷ The fractions enriched in coated vesicles were pooled, diluted tenfold with isolation buffer, and centrifuged for 10 min at 10,000g; the supernatant containing coated vesicles was used for subsequent analysis within one day after purification. Frozen hydrated samples of clathrin-coated vesicles were prepared by applying a 2.5 μl drop of sample (a protein concentration of about 1 mg/ml) to a glow-discharged 200-mesh Quantifoil holey carbon grid (Quantifoil Micro Tools GmbH, Germany). Before plunging the grid into liquid ethane at -180 °C, 1 μl of 10 nM colloidal gold particles (BBInternational, UK) was added to the sample,

followed by blotting with filter-paper. A tilt series of 62 images from -55° to +67° with 2° increments was collected using a Tecnai F20 field-emission microscope (FEI company, USA) operated at an acceleration voltage of 200 kV. Following strict low-dose procedures, images of the tilt series were recorded manually at a nominal magnification of 29,000× on a 2K×2K CCD camera with the defocus set to -7 μm. The electron dose used for collecting each image of the tilt series was 1.5 e⁻/Å², and the total electron dose for the series was about 100 e⁻/Å²; the total dose used for tracking during the data collection was only about 0.5 e⁻/Å². The particles were clearly visible even in the last image of the tilt series (Figure 1(d)), and there was no evident radiation-induced bubbling. All the images were binned 2×2 before further processing, corresponding to a final calibrated pixel size of 15.5 Å/pixel.

Image processing

The program package IMOD was used to process the images of the tomographic tilt series.²⁴ After initial coarse alignment using cross-correlation between images from different tilt angles, 44 colloidal gold particles were selected as fiducial markers to align all the images of the tilt series. The thickness of the calculated tomogram was 100 pixels (~1550 Å), corresponding to the thickness of the layer of vitreous ice. No segmentation, either manual or automated, was performed to interpret the cryo-electron tomogram. Individual assemblies were boxed out from the 3D reconstructed tomogram using the program label.exe in the MRC package.²⁵ Noise in the boxed-out 3D density maps was reduced by a 3×3×3 median filter.²⁶

Structure analysis

The program O was used to analyze the individual coats.²⁷ An artificial multi-Ala α-helix was used as a fiducial to mark the edges of the clathrin lattice and ultimately to draw its outlines as shown in Figure 4(b). Views of the 3D density maps were prepared for illustration using the program Chimera.²⁸

Acknowledgements

This work was supported by National Institutes of Health grant GM62580 (to David DeRosier) and GM36548 (to T.K.). The molecular EM facility at Harvard Medical School was established by a generous donation from the Giovanni Armenise Harvard Center for Structural Biology.

References

1. Kirchhausen, T. (2000). Clathrin. *Annu. Rev. Biochem.* **69**, 699–727.
2. Brodsky, F. M., Chen, C. Y., Knuehl, C., Towler, M. C. & Wakeham, D. E. (2001). Biological basket weaving: formation and function of clathrin-coated vesicles. *Annu. Rev. Cell Dev. Biol.* **17**, 517–568.
3. Sudhof, T. C. (2004). The synaptic vesicle cycle. *Annu. Rev. Neurosci.* **27**, 509–547.

4. Crowther, R. A., Finch, J. T. & Pearse, B. M. (1976). On the structure of coated vesicles. *J. Mol. Biol.* **103**, 785–798.
5. Kirchhausen, T. & Harrison, S. C. (1981). Protein organization in clathrin trimers. *Cell*, **23**, 755–761.
6. Ungewickell, E. & Branton, D. (1981). Assembly units of clathrin coats. *Nature*, **289**, 420–422.
7. Conner, S. D. & Schmid, S. L. (2003). Regulated portals of entry into the cell. *Nature*, **422**, 37–44.
8. Ehrlich, M., Boll, W., Van Oijen, A., Hariharan, R., Chandran, K., Nibert, M. L. & Kirchhausen, T. (2004). Endocytosis by random initiation and stabilization of clathrin-coated pits. *Cell*, **118**, 591–605.
9. Vigers, G. P., Crowther, R. A. & Pearse, B. M. (1986). Three-dimensional structure of clathrin cages in ice. *EMBO J.* **5**, 529–534.
10. Smith, C. J., Grigorieff, N. & Pearse, B. M. (1998). Clathrin coats at 21 Å resolution: a cellular assembly designed to recycle multiple membrane receptors. *EMBO J.* **17**, 4943–4953.
11. Musacchio, A., Smith, C. J., Roseman, A. M., Harrison, S. C., Kirchhausen, T. & Pearse, B. M. (1999). Functional organization of clathrin in coats: combining electron cryomicroscopy and X-ray crystallography. *Mol. Cell*, **3**, 761–770.
12. Fotin, A., Cheng, Y., Sliz, P., Grigorieff, N., Harrison, S. C., Kirchhausen, T. & Walz, T. (2004). Molecular model for a complete clathrin lattice from electron cryomicroscopy. *Nature*, **432**, 573–579.
13. ter Haar, E., Musacchio, A., Harrison, S. C. & Kirchhausen, T. (1998). Atomic structure of clathrin: a beta propeller terminal domain joins an alpha zigzag linker. *Cell*, **95**, 563–573.
14. Ybe, J. A., Brodsky, F. M., Hofmann, K., Lin, K., Liu, S. H., Chen, L. *et al.* (1999). Clathrin self-assembly is mediated by a tandemly repeated superhelix. *Nature*, **399**, 371–375.
15. Fotin, A., Cheng, Y., Grigorieff, N., Walz, T., Harrison, S. C. & Kirchhausen, T. (2004). Structure of an auxilin-bound clathrin coat and its implications for the mechanism of uncoating. *Nature*, **432**, 649–653.
16. Matsui, W. & Kirchhausen, T. (1990). Stabilization of clathrin coats by the core of the clathrin-associated protein complex AP-2. *Biochemistry*, **29**, 10791–10798.
17. Woodman, P. G. & Warren, G. (1991). Isolation of functional, coated, endocytic vesicles. *J. Cell Biol.* **112**, 1133–1141.
18. Pearse, B. M. & Crowther, R. A. (1987). Structure and assembly of coated vesicles. *Annu. Rev. Biophys. Biophys. Chem.* **16**, 49–68.
19. Baumeister, W. (2005). From proteomic inventory to architecture. *FEBS Letters*, **579**, 933–937.
20. Heuser, J. (1980). Three-dimensional visualization of coated vesicle formation in fibroblasts. *J. Cell Biol.* **84**, 560–583.
21. Maycox, P. R., Link, E., Reetz, A., Morris, S. A. & Jahn, R. (1992). Clathrin-coated vesicles in nervous tissue are involved primarily in synaptic vesicle recycling. *J. Cell Biol.* **118**, 1379–1388.
22. Perry, M. M. & Gilbert, A. B. (1979). Yolk transport in the ovarian follicle of the hen (*Gallus domesticus*): lipoprotein-like particles at the periphery of the oocyte in the rapid growth phase. *J. Cell Sci.* **39**, 257–272.
23. Schikorski, T. & Stevens, C. F. (1997). Quantitative ultrastructural analysis of hippocampal excitatory synapses. *J. Neurosci.* **17**, 5858–5867.
24. Kremer, J. R., Mastronarde, D. N. & McIntosh, J. R. (1996). Computer visualization of three-dimensional image data using IMOD. *J. Struct. Biol.* **116**, 71–76.
25. Crowther, R. A., Henderson, R. & Smith, J. M. (1996). MRC image processing programs. *J. Struct. Biol.* **116**, 9–16.
26. Winkler, H. & Taylor, K. A. (2006). Accurate marker-free alignment with simultaneous geometry determination and reconstruction of tilt series in electron tomography. *Ultramicroscopy*, **106**, 240–254.
27. Jones, T. A., Zou, J. Y., Cowan, S. W. & Kjeldgaard (1991). Improved methods for building protein models in electron density maps and the location of errors in these models. *Acta Crystallog. sect. A*, **47**, 110–119.
28. Pettersen, E. F., Goddard, T. D., Huang, C. C., Couch, G. S., Greenblatt, D. M., Meng, E. C. & Ferrin, T. E. (2004). UCSF Chimera—A visualization system for exploratory research and analysis. *J. Comput. Chem.* **25**, 1605–1612.
29. Heldwein, E. E., Macia, E., Wang, J., Yin, H. L., Kirchhausen, T. & Harrison, S. C. (2004). Crystal structure of the clathrin adaptor protein 1 core. *Proc. Natl Acad. Sci. USA*, **101**, 14108–14113.

Edited by W. Baumeister

(Received 1 August 2006; received in revised form 24 September 2006; accepted 5 October 2006)

Available online 14 October 2006